Am J Physiol Lung Cell Mol Physiol 290: L200–L208, 2006.
First published August 19, 2005; doi:10.1152/ajplung.00186.2005.

NO responsiveness in pulmonary artery and airway smooth muscle: the role of cGMP regulation

Young L. Kwak,[2] Keith A. Jones,[1] David O. Warner,[1] and William J. Perkins[1]

[1]*Departments of Anesthesiology, and Physiology and Biophysics, Mayo Clinic College of Medicine, Rochester, Minnesota; and* [2]*Department of Anesthesia and Pain Medicine, Yonsei University College of Medicine, Seoul, Korea*

Submitted 25 April 2005; accepted in final form 12 August 2005

Kwak, Young L., Keith A. Jones, David O. Warner, and William J. Perkins. NO responsiveness in pulmonary artery and airway smooth muscle: the role of cGMP regulation. *Am J Physiol Lung Cell Mol Physiol* 290: L200–L208, 2006. First published August 19, 2005; doi:10.1152/ajplung.00186.2005.—The purpose of this study was to assess intrinsic smooth muscle mechanisms contributing to greater nitric oxide (NO) responsiveness in pulmonary vascular vs. airway smooth muscle. Canine pulmonary artery smooth muscle (PASM) and tracheal smooth muscle (TSM) strips were used to perform concentration response studies to an NO donor, (Z)-1-[N-(2-aminoethyl)-N-(2-ammonioethyl)amino]diazen-1-ium-1,2-diolate (DETA-NO). PASM exhibited a greater NO responsiveness whether PASM and TSM were contracted with receptor agonists, phenylephrine and acetylcholine, respectively, or with KCl. The >10-fold difference in NO sensitivity in PASM was observed with both submaximal and maximal contractions. This difference in NO responsiveness was not due to differences in endothelial or epithelial barriers, since these were removed, nor was it due to the presence of cGMP-independent NO-mediated relaxation in either tissue. At equal concentrations of NO, the intracellular cGMP concentration ($[cGMP]_i$) was also greater in PASM than in TSM. Phosphodiesterase (PDE) inhibition using isobutylmethylxanthine indicated that the greater $[cGMP]_i$ in PASM was not due to greater PDE activity in TSM. Expression of soluble guanylate cyclase (sGC) subunit mRNA (2 ± 0.2 and 1.3 ± 0.2 attomol/μg total RNA, respectively) and protein (47.4 ± 2 and 27.8 ± 3.9 ng/mg soluble homogenate protein, respectively) was greater in PASM than in TSM. $sGC\alpha_1$ and $sGC\beta_1$ mRNA expression was equal in PASM but was significantly different in TSM, suggesting independent regulation of their expression. An intrinsic smooth muscle mechanism accounting for greater NO responsiveness in PASM vs. TSM is greater sGC activity.

nitric oxide; soluble guanylate cyclase; guanosine 3′,5′-cyclic monophosphate; phosphodiesterase; pulmonary artery; airway smooth muscle; molecular sequence data

AIRWAY SMOOTH MUSCLE APPEARS to be less responsive to exogenously administered nitric oxide (NO) and NO donors than the pulmonary arterial circulation (6). For example, concentrations of inhaled NO that reduce pulmonary vascular resistance have only a slight beneficial effect in cases of symptomatic airway constriction (19, 21). Similarly, intravenous administration of NO donors temporarily reduces systemic and pulmonary arterial vascular resistance but has not been notably effective in the treatment of airway constriction (24). There are a variety of reasons that could contribute to differences in NO responsiveness in smooth muscle in the pulmonary vasculature and airways, including differences in the barriers separating the underlying smooth muscle from exogenously administered NO (27) and differences in the NO response system in smooth muscle from the two tissues. The present studies focus on intrinsic smooth muscle contributions from these two tissues to differences in NO responsiveness.

The primary initial enzyme in the smooth muscle NO response system is soluble guanylate cyclase (sGC) (18, 33). Active sGC usually exists as a heterodimer of two subunits, primarily $sGC\alpha_1$ and $sGC\beta_1$, in vascular smooth muscle, although other subunits are known to exist, including $sGC\alpha_2$, $sGC\alpha_{2i}$, and $sGC\beta_2$. These subunits can form other active heterodimers (14, 49), some of which have lower NO inducible activity. sGC activity is significantly increased by NO binding at the sGCβ subunit heme (46) to catalyze the conversion of guanosine 5′-triphosphate to guanosine 3′,5′-cyclic monophosphate (cGMP). Homodimers of sGC (e.g., $sGC\beta_1/sGC\beta_1$) can form but have no activity (48), indicating that while only one subunit is involved in NO binding, both subunits are required in the dimer for enzyme activity (5). The finding that sGC homodimers form in expression systems raises the possibility that they may also exist in tissues expressing this enzyme. Intracellular cGMP concentration ($[cGMP]_i$) is also regulated by calmodulin-dependent and -independent phosphodiesterases (PDE), with roughly equal contributions from both classes of PDE in pulmonary artery (29, 38). $[cGMP]_i$ plays a variety of roles in the smooth muscle cell, most of them mediated by cGMP-dependent protein kinases (cGK) with the salient cGMP/cGK-mediated mechanism for smooth muscle relaxation related to reductions in myoplasmic Ca^{2+} (13) and sensitivity of the myofilament contractile proteins to Ca^{2+} (37, 40, 42). Differences in the NO response system in smooth muscle may thus exist at the level of cGMP production (i.e., sGC activity), PDE-mediated cGMP breakdown, and cGMP responsiveness. Smooth muscle in both the pulmonary vasculature and airways contains the enzymes necessary to transduce NO signaling, including sGC (4, 6, 11, 43) and cGK (1, 9, 10, 12, 36, 47), although the level of sGC and cGK expression in these tissues has not been quantified.

In the present study, we determined the effects of NO on tissue $[cGMP]_i$ and relaxation following a standardized contraction in pulmonary artery and airway smooth muscle [pulmonary artery smooth muscle and tracheal smooth muscle (PASM and TSM, respectively)]. We tested the hypothesis that the NO responsiveness of PASM is greater than that of TSM in part because of greater protein expression of sGC in the former tissue, consequently producing higher tissue cGMP at a given

Address for reprint requests and other correspondence: W. J. Perkins, Mayo Clinic College of Medicine, 200 1st St., SW, Rochester, MN 55905 (e-mail: perkinsw@mayo.edu).

The costs of publication of this article were defrayed in part by the payment of page charges. The article must therefore be hereby marked "*advertisement*" in accordance with 18 U.S.C. Section 1734 solely to indicate this fact.

NO concentration. In the course of these studies, the types and levels of sGC subunit expression were semiquantitatively determined in these tissues for the first time.

MATERIALS AND METHODS

Tissue preparation. After Institutional Animal Care and Use Committee approval, mongrel dogs of either sex were anesthetized with an intravenous injection of pentobarbital sodium (30 mg/kg) and exsanguinated by bilateral transection of the carotid arteries. The trachea and lungs were excised and immersed in chilled physiological salt solution (PSS) of the following composition (in mM): 110 NaCl, 26 $NaHCO_3$, 5.6 dextrose, 3.4 KCl, 2.4 $CaCl_2$, 1.2 KH_2PO_4, and 0.8 $MgSO_4$. Third-generation pulmonary artery was dissected from the lung parenchyma, cut into rings, and cleaned of adventitia under microscopic observation, and the endothelium was removed by gentle rubbing of the luminal surface with a moist cotton swab. The fat, connective tissue and the epithelium were removed with tissue forceps and scissors under microscopic observation to make muscle strips.

The NO responsiveness of first- to fourth-generation pulmonary artery was not significantly different (unpublished observations), and third-generation pulmonary artery was used in these studies due to ease of preparation and definition of myocyte orientation. Higher-generation airways were not used due to difficulties in separating epithelial cells from smooth muscle cells, which was undesirable in the biochemical and expression studies.

Mechanical measurements. TSM and PASM strips were mounted in 5-ml water-jacketed tissue baths that were filled with PSS (37°C) aerated with O_2/CO_2, 94%:6%, pH 7.4. One end of the strips was anchored to metal hooks at the bottom of the tissue bath; the other end was attached to a calibrated force transducer (model FT03D; Grass Instruments/Astro-Med, West Warwick, RI). During a 3-h equilibration period, the strips were repeatedly contracted isometrically with 40 mM KCl and then relaxed. The length of the strips was increased after each contraction-relaxation cycle until active force was maximal (optimal length). Relaxed PA strips were then contracted with norepinephrine (1 μM), and the absence of endothelium was verified by failure of acetylcholine (1 μM) to cause relaxation. Strips were then relaxed again until commencement of a study. Before concentration-response studies, all strips were incubated with 10 μM indomethacin to prevent the formation of prostanoids. In previous studies, contraction of TSM and PASM during incubation with indomethacin had no effect on tissue $[cGMP]_i$ (20).

Concentration-response curves. Concentration responses to the NO donor in TSM and PASM were obtained 15 min following an isometric contraction using either a physiological contractile agonist or KCl. The contractile agonists used were acetylcholine and phenylephrine for TSM and PASM, respectively. The NO donor (Z)-1-[N-(2-aminoethyl)-N-(2-ammonioethyl)amino]diazen-1-ium-1,2-diolate (DETA-NO) was selected since it slowly releases NO (23), giving rise to stable relaxations at a given [DETA-NO], and does not require biotransformation to release NO (30). DETA-NO concentration response studies were performed with contractile agonists and KCl to test for the possibility that any difference in DETA-NO response could be attributed to differences in contractile mechanism between TSM and PASM. DETA-NO concentration response curves were performed under conditions of both maximal and submaximal contraction for both contractile agonists and KCl. We determined submaximal concentrations of both contractile agonist and KCl by initially contracting the strip to maximal isometric force, allowing it to fully relax after washout and adding contractile agent until the isometric force attained 50 ± 10% of the maximal value. In the initial experiment, the effects of 10 μM sGC inhibitor 1*H*-[1,2,4]Oxadiazole[4,3-a]quinoxalin-1-one (ODQ) and 100 μM β-phenyl-1,N^2-etheno-8-bromoguanosine-3′,5′-cyclic monophosphorothioate, Rp-isomer, a membrane-permeant, phosphodiesterase-resistant cGMP-dependent protein kinase inhibitor (cGKi), on DETA-NO-induced relaxation was examined to assess the presence of cGMP- or cGK-independent relaxation. Studies were done at both maximal and submaximal isometric force to determine whether the DETA-NO concentration response was sensitive to the degree of smooth muscle activation. In all concentration-response curves, the relaxation is indexed to the isometric force obtained just before the addition of DETA-NO (control condition) and is expressed as a percentage of control.

Cyclic nucleotide measurements. TSM and PASM strips were incubated in 10-ml baths and aerated with PSS at 37°C. Strips were treated with a stated concentration of DETA-NO in the presence or absence of 500 μM isobutylmethylxanthine (IBMX) and were then snap frozen with liquid nitrogen and stored in a −70°C freezer. Strips were then homogenized, and the soluble extract was assayed for cGMP with a commercially available RIA kit (Amersham Biosciences) as previously described (39). The protein concentration in the tissue homogenate was determined by the method described by Lowry et al. (28), using bovine serum albumin dissolved in 1 N NaOH as the standard. Tissue $[cGMP]_i$ was expressed in pmol/mg protein. Strips treated with IBMX were incubated with this agent for 10 min before the addition of DETA-NO. Two sets of experiments were performed. The first examined the time course of increases in $[cGMP]_i$ following addition of DETA-NO to both tissues. The second used this information to select the sample time for examining the effects of DETA-NO, IBMX, and IBMX + DETA-NO on $[cGMP]_i$ accumulation in both tissues.

sGC subunit sequencing. Total RNA was prepared from RNAlater (Ambion, Austin, TX)-treated TSM and PASM tissue by extraction with guanidinium isothiocyanate and subsequent sedimentation through CsCl (8). RNA quality was assessed by RNA electrophoresis on an agarose gel. Only samples in which the ratio of 28S/18S ribosomal RNA bands was at least >1.2 and with little evidence of laddering below or between these bands were studied. mRNA was isolated from total RNA using Micro-Fast Track (Invitrogen, Carlsbad, CA) and was then reverse transcribed using avian myeloblastosis virus reverse transcriptase (Clontech, Mountain View, CA). The resulting single-stranded cDNA was probed by rapid amplification of cDNA ends (Clontech), using adapter sequences and a sequence for the sGC subunit that was highly conserved across species. For $sGC\alpha_1$, nucleotides 2198–2200 of the rat sequence (34) (accession no. M36075) and, for $sGC\beta_1$, nucleotides 1701–1679 of the human sequence (17) (antisense, accession no. X66533) were used as the initial probes for touchdown PCR. The resulting cDNA band was purified from an agarose gel and subcloned into pCR2.1 vector using TOPO TA cloning kit (InVitrogen). Positive *Escherichia coli* colonies were tested for the insert with colony PCR using M13 forward and reverse primers. Plasmid containing the insert was purified from a broth culture of a positive colony using Wizard plasmid miniprep (Promega, Madison, WI). The sequence of the insert was initially characterized with M13 forward and M13 reverse primers by the Sanger dideoxy method (41) at the Mayo Rochester DNA Sequencing and Synthesis Core Facility (Rochester, MN). These sequences were used to generate new primers to extend the sequence until the complete open frame was obtained. Overlapping sequences were used to design gene-specific sequencing primers for obtaining the full-length open reading frame sequence of each sGC subunit in triplicate. The resulting canine $sGC\alpha_1$ and $sGC\beta_1$ sequences were submitted to the National Center for Biotechnology Information and have accession numbers DQ008575 and DQ008576, respectively. Oligonucleotide probes and primers were synthesized at the Mayo Rochester Core Facility. Oligonucleotide primers designed on the basis of published sequences were used to probe for $sGC\alpha_2$, $sGC\alpha_{2i}$, and $sGC\beta_2$ subunit isoforms (accession nos. X63282, Z50053, and M57507, respectively).

Measurement of sGC mRNA expression. cDNA was prepared from total RNA from tissues taken from separate animals and stored at −20°C until the time for determination of sGC subunit cDNA

concentration. Quantitative RT-PCR was used for this determination (2, 16). The exogenous internal standards (mimes) were derived from pBR322 and composite primers for PCR amplifying these were produced as described in Table 1. The pBR322 sequence was selected to have a melting point by nearest neighbor estimation (Oligo Software, Cascade, CO) within 2°C of the sGC subunit sequence being amplified. The respective size of the mime-sGC amplicon sequences were 345:225 and 348:398 bp for $sGC\alpha_1$ and $sGC\beta_1$, respectively. The amplified mime sequences were purified and subcloned into pCR2.1 plasmid using TOPO TA cloning (Invitrogen), and colonies containing the mime insert were selected as described above in *sGC subunit sequencing*. Plasmid was purified from the *E. coli* pellet using a QIAfilter Plasmid Maxi Kit (Qiagen, Valencia, CA). Confirmation of insertion was obtained by sequencing the plasmid and testing for amplification with sGC subunit-selective primers. Plasmid and mime concentrations were quantitated using optical density at 260 nm. Mime cDNA concentrations for determination of sGC cDNA concentration in total RNA from TSM and PASM were 0.01, 0.025, 0.05, 0.1, 0.25, and 0.5 amol for both sGC subunits. Samples underwent PCR for 30 cycles with the following cycling conditions: 30 s initial denaturation at 94°C, followed by 25 cycles of 10 s denaturation at 94°C, and 2 min 30 s annealing and extension at 68°C with a final extension at 72°C for 3 min. The PCR products were run on a 2.5% composite agarose gel [1.5% LMP Ultrapure agarose + 1% Ultrapure agarose (Invitrogen)] containing 500 ng/ml ethidium bromide for staining. Gels were digitized using an AlphaInnotech ChemImager400 imaging system, and the resulting images were analyzed with Optiquant software (PerkinElmer, Boston, MA). The amount of gene-specific mRNA was determined by linear regression analysis of a plot of log [intensity mime/intensity sample] vs. log [moles mime in PCR reaction]. The point at which the regression line crosses 0 on the *y*-axis determines the number of moles of sGC subunit mRNA present in the original total RNA sample. The quantity of gene-specific mRNA is expressed in amol/μg total RNA.

Measurement of sGC protein expression. TSM and PASM strips, 10–20 mg wet weight, were flash frozen by rapid immersion in a dry ice-acetone slurry. The tissue strips were then placed in homogenizing tubes and homogenized in the presence of 100 μl of extraction buffer (in mM, 10 Tris·HCl, 150 NaCl, 10 dithiothreitol, 1 Na_2EDTA, 1 phenylmethylsulfonyl fluoride, 1 benzamidine, and 10 μg/ml leupeptin, aprotinin, pepstatin Am, and antipain, pH 7.4). The tubes were then centrifuged at 4,000 *g* for 10 min to pellet solids. Protein concentration in the supernatant was determined by the Lowry method. Approximately 20 μg of protein in Laemmli buffer (Bio-Rad) were loaded per lane. Known amounts of purified sGC protein (Alexis Biochemicals, Lausen, Switzerland) were loaded in adjacent lanes to generate a standard curve. Proteins were separated by electrophoresis in SDS-7.5% polyacrylamide precast minigels (Bio-Rad) with Tris-Glycine-SDS buffer. The proteins were transferred to a polyvinylidene difluoride membrane in Tris-Glycine buffer for 45 min at 100 V, and the membrane was washed with 10 mM Tris-buffered saline containing 5% (wt/vol) bovine serum albumin for 15 min (25°C). The membrane was then treated with Tris-buffered saline containing 0.2% Tween 20 and 1:10,000 dilution of sGC polyclonal rabbit antibody (Cayman Chemical, Ann Arbor, MI) overnight. After being washed, the membrane was treated with 1:10,000 anti-rabbit horseradish peroxidase-conjugated IgG antibody (Santa Cruz Biotechnology, Santa Cruz, CA) for 30 min and then washed again. Membranes were then treated with enhanced chemiluminescence Western blotting reagents (ECL; Amersham, Piscataway, NJ) for 1 min, apposed to Kodak BioMax film, and developed for a period of time that avoided saturation of any bands. The film was scanned and digitized with Adobe Photoshop and subsequently analyzed with Optiquant software (Packard Instruments).

Materials. DETA-NO, ODQ, and β-phenyl-1,N^2-etheno-8-bromoguanosine-3′,5′-cyclic monophosphorothioate, Rp-isomer, a membrane-permeant, phosphodiesterase-resistant cGKi were purchased from Alexis Biochemicals. Unless otherwise specified, all other chemicals were purchased from Sigma-Aldrich (St. Louis, MO). With the exception of ODQ and cGKi, which were dissolved in 50% DMSO, all drugs and chemicals were dissolved in distilled water.

Analysis of data. Data are expressed as means ± SE; *n* represents the number of dogs. The effects of DETA-NO on isometric force and $[cGMP]_i$ were assessed by repeated-measures ANOVA with post hoc analysis by Duncan's multiple-range test. Concentration-response curves were compared by nonlinear regression analysis as described by Meddings et al. (31). In this method, force (F) at any concentration of drug (C) is given by the equation $F = F_mC/(EC_{50} + C)$, where F_m represents the maximal isometric force and EC_{50} represents the concentration that produces half-maximal isometric force for that drug. Nonlinear regression analysis was used to fit values of F_m and EC_{50} to data for F and C for each condition studied. This method allows comparison of curves to determine whether they are significantly different and whether this overall difference can be attributed to differences in F_m, EC_{50}, or both parameters. A P value <0.05 was considered statistically significant.

RESULTS

Physiological studies. In both PASM and TSM, following an initial submaximal contraction with ~25 mM KCl and 15-min treatment with the specified inhibitors, the relaxation to DETA-NO was stable (data not shown) at each concentration and was complete at the highest concentration. DETA-NO-induced relaxation was significantly decreased by 10 μM ODQ, an sGC inhibitor, and 30 μM cGKi and was completely inhibited by the combination of the sGC and cGKi, except at the 10^{-4} DETA-NO concentration in PASM (Fig. 1). The addition of ODQ, cGKi, and DMSO alone (<0.2%) had no effect on KCl-induced contractions in PASM or TSM (data not shown).

Phenylephrine (10 μM) and acetylcholine (1 μM) produced maximal isometric force in PASM and TSM, respectively (data

Table 1. *Composite primer sequences*

Subunit	Sequence	Nucleotide No. sGC	Nucleotide No. pBR322
$sGC\alpha_1$			
Sense	GGTTGTGCAAGCCAAGAAGTTCAG**GATCGTTGTCAGAAGTAAGTTGG**	1770–1794	3734–3756
Antisense	GGGTGTCACTTTCTTTGTGCAATCC**GGGTTACATCGAACTGGATCTC**	1994–1970	4028–4007
$sGC\beta_1$			
Sense	GATACAATCTTGCGTGTCCTGGGATC**GATCGTTGTCAGAAGTAAGTTGG**	271–296	3734–3756
Antisense	GCTTTGCAGAAGGTATATGGGCTGATG**GGGTTACATCGAACTGGATCTC**	668–642	4028–4007

Composite primer sequences showing sequences used to probe for soluble guanylate cyclase (sGC) subunit cDNA and mime constructed from sGC subunit sequence + specified (bold) pBR322 sequence.

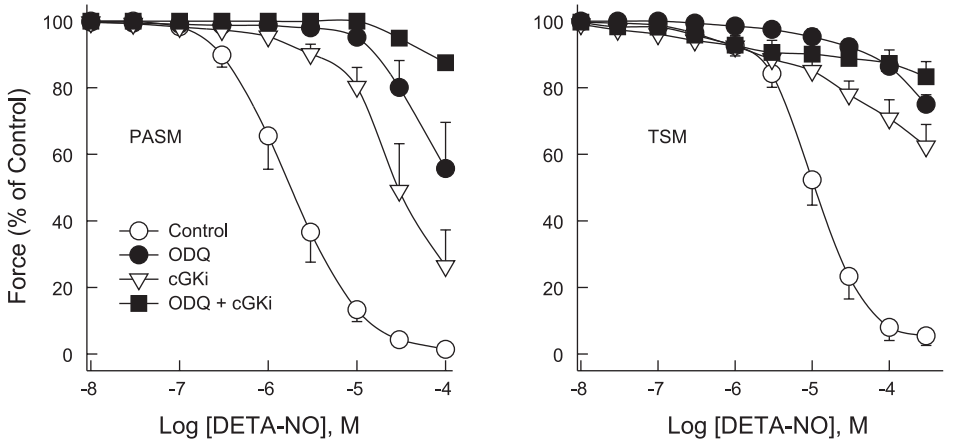

Fig. 1. Effects of the nitric oxide (NO) donor (Z)-1-[N-(2-aminoethyl)-N-(2-ammonioethyl)-amino]diazen-1-ium-1,2-diolate (DETA-NO) on isometric force in pulmonary artery smooth muscle (PASM, *left*) and tracheal smooth muscle (TSM, *right*). Strips were contracted to half-maximal isometric force with KCl. DETA-NO concentration response curves were obtained without (Control) and with 10 μM soluble guanylate cyclase inhibitor 1H-[1,2,4]Oxadiazole[4,3-a]quinoxalin-1-one (ODQ), 100 μM β-phenyl-1,N^2-etheno-8-bromoguanosine-3′,5′-cyclic monophosphorothioate, Rp-isomer, a cGMP-dependent protein kinase inhibitor (cGKi), and both inhibitors (ODQ + cGKi). Data are presented as means ± SE; $n = 6$.

not shown). In the presence of agonists sufficient to achieve ~50% maximal isometric force (~0.2 μM phenylephrine and 0.1 μM acetylcholine), DETA-NO produced complete relaxation (Fig. 2, *left*). The log EC_{50} for DETA-NO was significantly less for PASM compared with TSM (−6.49 ± 0.13 and −5.24 ± 0.12 M, respectively; $P < 0.001$). A similar pattern of results was observed during maximal contractions with agonists (log EC_{50} for DETA-NO in PASM and TSM of −6.09 ± 0.08 and −4.7 ± 0.08 M, respectively; $P < 0.001$) (Fig. 2, *right*). DETA-NO produced complete relaxation of maximally contracted PASM and TSM.

Maximal isometric force in response to KCl in PASM and TSM was achieved with 40 and 60 mM KCl, respectively (data not shown). During KCl activation achieving ~50% maximal isometric force (requiring 25 and 21 mM for PASM and TSM, respectively) DETA-NO produced complete relaxation of both tissues (Fig. 3, *left*). The log EC_{50} for DETA-NO was less in PASM and TSM (−5.73 ± 0.11 and −4.99 ± 0.96 M, respectively; $P < 0.001$). A similar pattern of results was observed during maximal contractions produced by KCl (log EC_{50} of 5.34 ± 0.13 and 4.44 ± 0.07, respectively; $P < 0.001$, Fig. 3, *right*). Relaxation to DETA-NO was incomplete during maximal KCl activation.

Tissue cGMP ($[cGMP]_i$) was slightly, but significantly, greater in PASM compared with TSM in the absence of DETA-NO (0.48 ± 0.04 and 0.30 ± 0.03 pmol/mg protein, respectively; $P = 0.008$, Fig. 4). No increase in $[cGMP]_i$ could be detected at ~EC_{50} (PASM and TSM) or EC_{90} (TSM). At 10 times EC_{90} DETA-NO $[cGMP]_i$ increased in both tissues within 30 s ($P < 0.001$). The $[cGMP]_i$ did not significantly change at 60 s or 15 min (Fig. 4).

DETA-NO at 10 μM (~EC_{90} in PASM and EC_{50} in TSM) produced an increase in $[cGMP]_i$ in PASM, but not in TSM (0.99 ± 0.10 and 0.36 ± 0.07 pmol/mg protein, $P < 0.001$). DETA-NO at 100 μM produced an increase in $[cGMP]_i$ in PASM and TSM (4.85 ± 0.69 and 1.44 ± 0.24 pmol/mg protein, respectively), and this increase was significantly greater in PASM ($P = 0.009$). Exposure to the general PDE inhibitor IBMX for 10 min slightly, but significantly, increased basal $[cGMP]_i$ in PASM, but not TSM. IBMX augmented the increases in $[cGMP]_i$ produced by 10 μM and 100 μM DETA-NO in both tissues (Fig. 5). This augmentation was

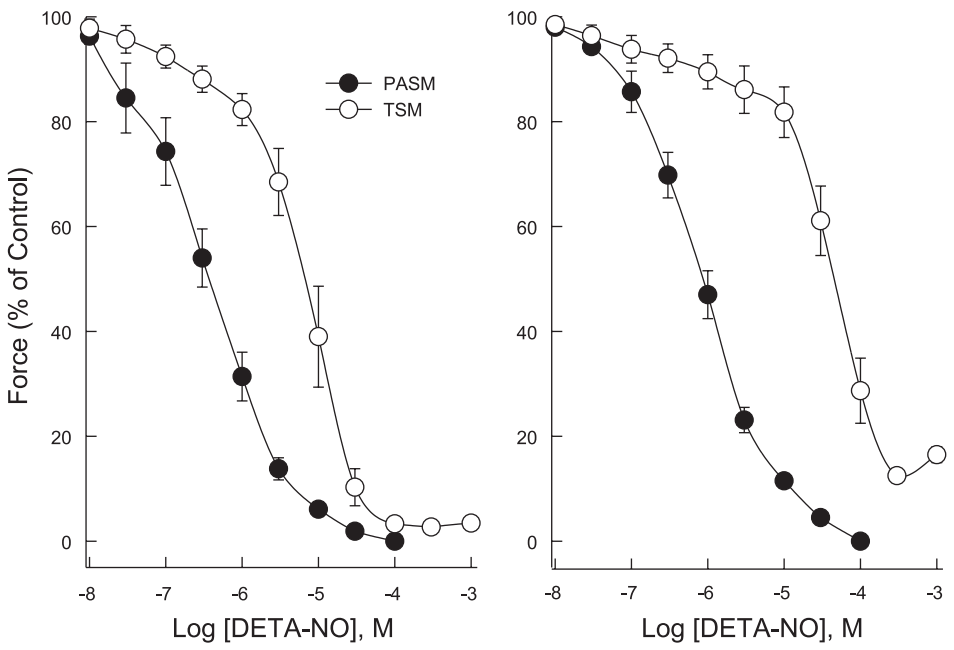

Fig. 2. Effects of the NO donor DETA-NO on isometric force in PASM and TSM strips contracted to half-maximal (*left*) and maximal (*right*) isometric force with phenylephrine in the case of PASM and acetylcholine in the case of TSM. Data are presented as means ± SE; $n = 6$.

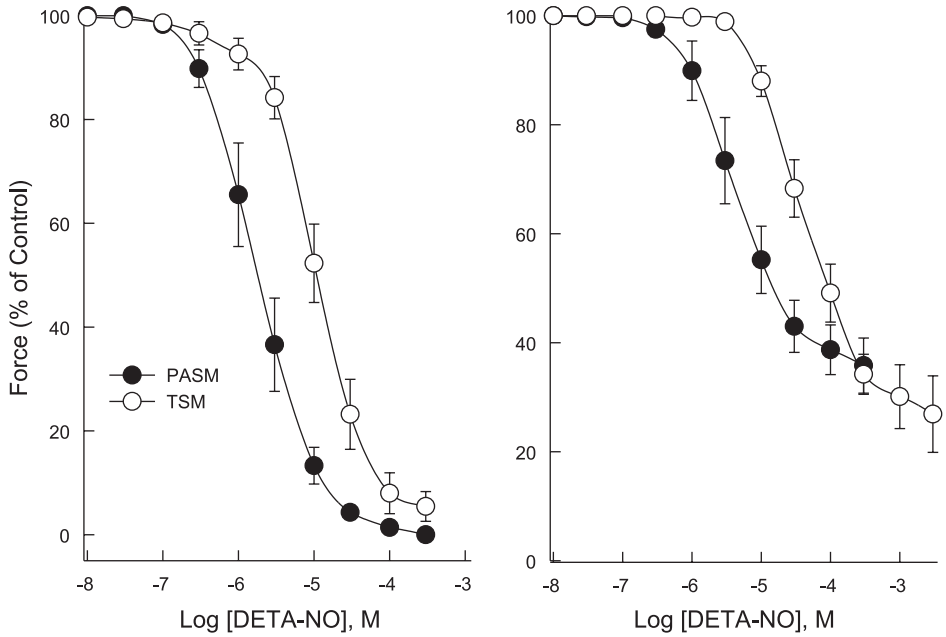

Fig. 3. Effects of the NO donor DETA-NO on isometric force in PASM and TSM contracted to half-maximal (*left*) and maximal (*right*) isometric force with KCl. Data are presented as means ± SE; $n = 6$.

greater for PASM than for TSM at both DETA-NO concentrations.

Expression studies. The mRNA sequence was determined for the sGC subunit sequences most abundantly expressed in these smooth muscle tissues. A very small amount of $sGC\alpha_2$ was found exclusively associated with PASM (<1% the amount of other subunits), but this was taken to be due to contamination from residual adventitia and was not further pursued. $sGC\alpha_2$, $sGC\alpha_{2i}$, and $sGC\beta_2$ mRNA expression was not detected in either tissue. Both $sGC\alpha_1$ and $sGC\beta_1$ were expressed at significant levels in both tissues and were sequenced through the complete open reading frame. In the open reading frame, $sGC\alpha_1$ was 88% homologous to the human and >90% homologous to rat and bovine $sGC\alpha_1$ sequences (accession nos. Y17523, M36075, and X54014, respectively). This sequence is identical to that predicted from genomic sequences for *Canis familiaris* (accession no. XM539780) with the exception of a 150-bp insert in the predicted sequence between nucleotides 2077 and 2078 in the sequence obtained in these studies. This insert would result in insertion of 50 amino acids between amino acids 572 and 573 of the inferred amino acid sequence. Such an insert is not present in $sGC\alpha_1$ mRNA sequences reported for other species. It is thus likely that the insert present in the genomically predicted sequence for $sGC\alpha_1$ in *C. familiaris* is intron sequence. The inferred $sGC\alpha_1$ amino acid homology and identity were ~95 and 90% for the human, rat, and bovine sequences.

The $sGC\beta_1$ mRNA sequence was >95% homologous with the human, rat, and bovine nucleotide sequences (accession

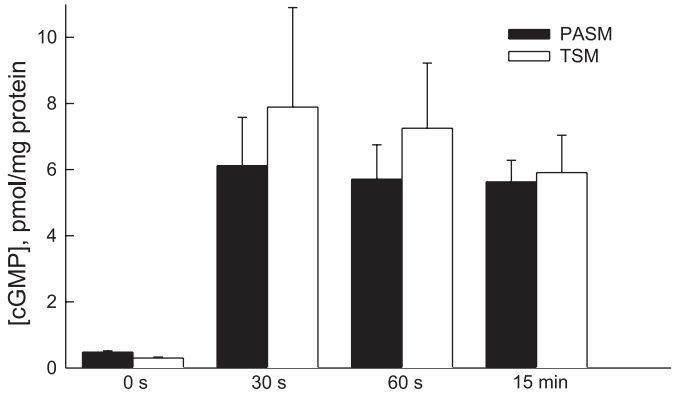

Fig. 4. Changes in intracellular cGMP concentration ($[cGMP]_i$) as a function of time following treatment of PASM (black) and TSM (white) with 100 and 500 μM NO donor DETA-NO, respectively. Data are presented as means ± SE, $n = 8$.

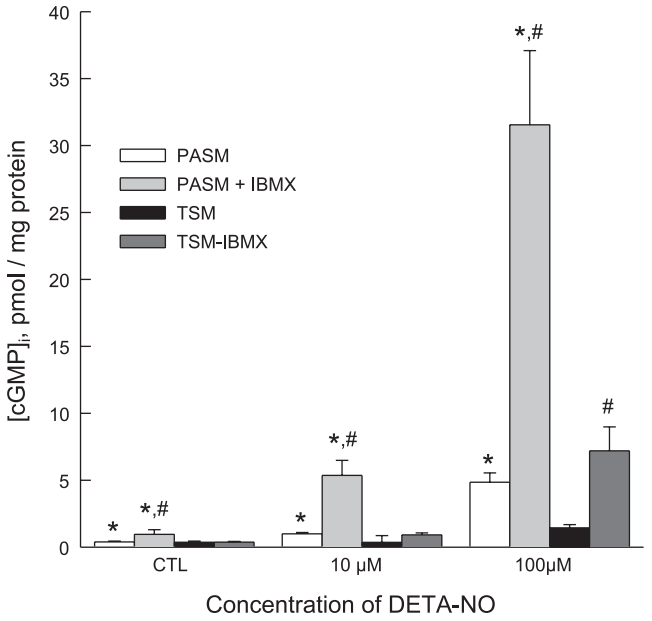

Fig. 5. Effects of isobutylmethylxanthine (IBMX, 500 μM) on intracellular cGMP ($[cGMP]_i$) measured 10 min after addition of the NO donor DETA-NO at the specified concentration to PASM and TSM. *Increase in $[cGMP]_i$ was greater in PASM vs. TSM at the specified condition, $P < 0.05$. #$[cGMP]_i$ differs significantly from the value obtained in the absence of IBMX, $P < 0.05$. Data are presented as means ± SE, $n = 8$.

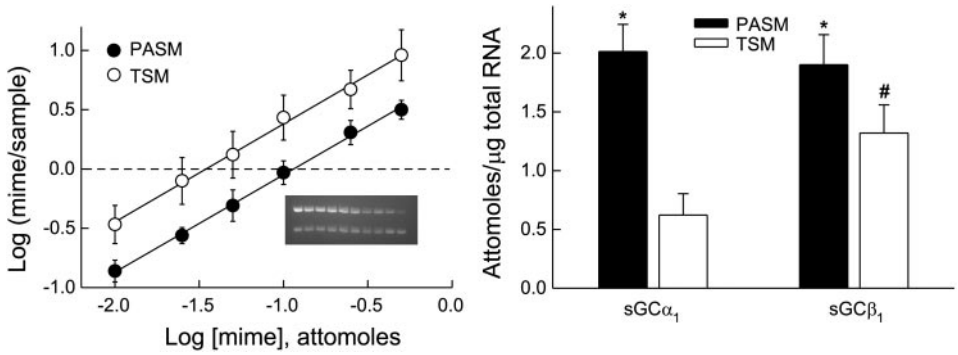

Fig. 6. Soluble guanylate cyclase (sGC) subunit mRNA expression in PASM and TSM by quantitative RT-PCR. *Left*: data illustrating the method for determining the amount of $sGC\alpha_1$ found in PASM and TSM. The dashed line indicates the point in the curves at which mime is equal to the sample, and this value is determined for each sample by interpolation. *Inset*: an example of an ethidium bromide agarose gel with mime cDNA bands above sample bands. *Right*: the amount of each sGC subunit mRNA present in PASM and TSM. *The amount of both sGC subunits is greater in PASM ($P < 0.025$). #The amount of $sGC\beta_1$ in TSM is greater than the amount of $sGC\alpha_1$ mRNA ($P < 0.05$). Data are presented as means ± SE, $n = 6$.

nos. X66533, M22562, and Y00770, respectively). The inferred amino acid homology and identity for this sGC subunit were 99 and 98% compared with the human, rat, and bovine inferred amino acid sequences. The predicted molecular weights of canine $sGC\alpha_1$ and $sGC\beta_1$ were 77,500 and 70,500, respectively.

The data set used to determine the mRNA expression for $sGC\alpha_1$ subunit is shown in Fig. 6, *left*. In this example, the plot of Log (mime/sample) vs. Log (mime) indicates that there is more $sGC\alpha_1$ in PASM than in TSM. The level of expression of both $sGC\alpha_1$ and $sGC\beta_1$ was greater ($P < 0.025$) in PASM, 2.0 ± 0.23 and 1.7 ± 0.2 amol/μg total RNA, respectively, than in TSM, 0.6 ± 0.2 and 1.3 ± 0.2, respectively (Fig. 6, *right*). The level of $sGC\alpha_1$ mRNA expression was significantly lower than that of $sGC\beta_1$ in TSM ($P < 0.05$), but expression of the two sGC subunits was equal in PASM.

An example of a purified sGC protein at six concentrations with equal loading of tissue homogenates from PASM and TSM on the same gel is shown in Fig. 7, *left*. A best-fit line was obtained with a sigmoidal curve, and the equation of this line was used to calculate the sGC protein concentration in the tissue homogenates. sGC protein expression was greater ($P < 0.001$) in PASM than in TSM, 47.4 ± 2 and 27.8 ± 3.9 ng/mg soluble homogenate protein (Fig. 7, *right*).

DISCUSSION

Relaxation to the NO donor DETA-NO occurs via the NO-cGMP signaling system in both PASM and TSM at all but the highest concentration of DETA-NO used in the pulmonary artery. The significant, but small, reduction in isometric force that occurred at 10^{-4} M DETA-NO in PASM either reflects the fact that the concentrations of the sGC and cGKi used do not completely overcome the effects of NO-mediated sGC activation at very high NO concentrations or that cGMP-independent relaxation becomes evident only at high NO concentrations. The observation that the combination of the sGC and cGKi prevented DETA-NO-induced relaxation to a greater extent than either agent alone suggests that the former explanation is more likely. The possibility that the difference in NO responsiveness between PASM and TSM is due to the presence of a significant cGMP-independent mechanism in one of them is thus unlikely. Although cGMP-independent relaxation to NO donors in TSM has been previously reported (39, 50), this was observed with a different class of NO donors, nitrosothiols and sodium nitroprusside. The present results corroborate those obtained using an NO donor and the sGC inhibitor ODQ in aortic rings and platelets (32). The finding that NO-mediated relaxations in both tissues are cGK dependent differs from

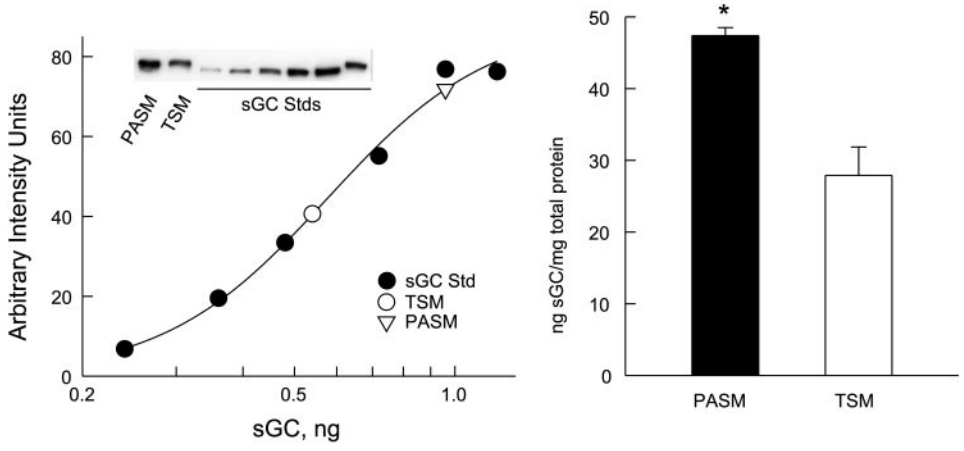

Fig. 7. The amount of sGC protein in the soluble fraction of tissue homogenates from PASM and TSM by a semiquantitative immunoblotting method. *Left*: representative data using known amounts of purified bovine lung sGC to create a standard curve (sGC Std) and 20 μg of homogenate from each tissue. *Inset*: representative experiment of an immunoblot used to generate the standard curve and tissue data points. *Right*: semiquantitative measurement of the amount of sGC in PASM and TSM. *The amount of sGC in PASM is greater than in TSM, $P < 0.001$. Data are presented as means ± SE, $n = 6$.

findings of a cGMP-dependent, cGK-independent NO donor-mediated relaxation in cat TSM (45), but this may be due to the use of a nitrosothiol NO donor or a species difference in the TSM preparation. Possible differences in bioconversion or permeability of the NO donor in PASM and TSM playing a role in NO responsiveness are also unlikely since DETA-NO does not require or undergo appreciable bioconversion to release NO (22, 23), which is highly membrane permeant.

TSM was less responsive to NO than PASM by more than an order of magnitude, under conditions that carefully matched the degree of agonist-induced contraction. Similar differences were observed regardless of the level of activation. The receptor-activated mechanisms used for the two different smooth muscle preparations were different, raising the possibility that the difference in NO responsiveness was due to differences in the receptor signaling giving rise to the initial contraction, although both agonists ultimately converge on a common pathway in which myoplasmic Ca^{2+} and Ca^{2+} sensitivity are increased (42). This is a possibly relevant consideration, since the mechanism by which cGMP and cGMP-dependent protein kinase decreases contraction in smooth muscle has not been clearly established. However, a similar pattern of results was found when membrane depolarization with KCl was used to induce contraction, suggesting that the observed difference between the two tissues does not depend upon the mechanism of contraction. Because KCl results in smooth muscle contraction predominantly by increasing calcium influx and $[Ca^{2+}]_i$, these results suggest that the difference in NO responsiveness between the two tissues is not due to differences in regulation of Ca^{2+} sensitivity, although more direct evidence would be required to demonstrate this. These results corroborate and extend previous results demonstrating a greater NO responsiveness in bovine pulmonary artery compared with TSM (6).

The EC_{50} concentration of DETA-NO in both tissues seems relatively high, between 10^{-6} and 10^{-5} M, but can be explained by the slow NO release kinetics, with a half-life of ~24 h at 37°C. An estimate of the NO concentration in the tissue bath, assuming apparent first-order kinetics for NO release and 2 NO released/DETA-NO, indicates that at 3 min, 10^{-6}–10^{-5} M DETA-NO results in 2.8–28 nM NO. Even this estimate is probably high, due to the fact that the bath system is open and bubbled with oxygen, which reacts with NO. The NO concentration resulting in 50% relaxation in PASM and TSM in the present study is thus likely lower than previously reported values using NO gas as the source (6, 43) and is in closer agreement with the potency of NO in inducing relaxation in vascular smooth muscle using flash photolysis on a membrane-permeant, photolabile NO-releasing compound (3, 7).

Addition of ~EC_{50} concentrations of the NO donor to the two tissues resulted in no detectable increase in $[cGMP]_i$, indicating that much of the relaxation to NO occurs with increases in cGMP that cannot be measured under steady-state conditions (i.e., in the absence of PDE inhibitors). Thus higher DETA-NO concentrations were used to determine the kinetics of $[cGMP]_i$ in the absence of PDE inhibitors. A rapid increase in $[cGMP]_i$ that did not significantly change after 30 s was observed in both tissues. This indicates that a steady-state condition in which cGMP production by sGC and breakdown by PDE is obtained rapidly in both tissues even at this relatively high NO donor concentration and is compatible with the stable relaxations obtained in both tissues with DETA-NO. It is interesting that nearly equipotent DETA-NO relaxant concentrations also had a similarly equipotent effect on $[cGMP]_i$. This suggests that the relationship between $[cGMP]_i$ and relaxation using this NO donor is similar between PASM and TSM, although this study does not systematically explore this relationship in either tissue.

Measurement of $[cGMP]_i$ in the presence and absence of the general PDE inhibitor IBMX demonstrated significant cGMP regulation in both tissues by PDE. IBMX, rather than a type V PDE-specific inhibitor, was selected since regulation of cGMP by PDE in PASM is not necessarily either type V selective or even predominant (29, 38). Although PDE types in airway smooth muscle have been explored (15, 44) the role of PDE types on cGMP conversion to GMP in TSM has not been determined. Thus the findings that the ratio of $[cGMP]_i$ obtained in the presence of DETA-NO with and without IBMX and the absolute increase in $[cGMP]_i$ with and without DETA-NO was greater in PASM than in TSM suggest that the lower $[cGMP]_i$ in TSM vs. PASM at a given NO donor concentration is not due to greater PDE-mediated cGMP breakdown in TSM. The results, in fact, suggest that PDE activity results in greater cGMP breakdown in PASM than in TSM, but a direct measurement of cGMP PDE activity in both tissues would be required to unambiguously demonstrate this.

The greater NO responsiveness of PASM vs. TSM is related in part to a greater increase in $[cGMP]_i$ induced by a given NO concentration. Because NO-induced cGMP production occurs exclusively via sGC, the results of these studies indicate that PASM must have greater sGC activity than TSM. Differences in sGC activity may be due to either increased expression of active sGC enzyme or increased sGC activity per unit of the enzyme present in the tissue (sGC-specific activity). Initial probing of both PASM and TSM for expression of sGC subunit mRNA indicated that only $sGC\alpha_1$ and $sGC\beta_1$ are significantly expressed in both tissues, the first time that this has been systematically determined in either smooth muscle tissue. It is therefore unlikely that specific activity regulation of sGC is due to expression of different sGC subunits in PASM and TSM. The levels of sGC subunit mRNA expression measured in these studies are the first semiquantitative report of their absolute, rather than relative, expression in smooth muscle tissues. The quantitative RT-PCR method used in these studies has the advantage of having an internal standard but may be limited in accuracy by variability in the quality of the mRNA in each preparation, the use of a cDNA rather than an RNA mime, and differences in the PCR efficiency between the mime insert sequence and the cDNA produced by reverse transcription of mRNA in a total RNA sample. Variability in the quality of RNA was assessed before the reverse transcription step, and RNA samples showing evidence of noticeable degradation were not reverse transcribed. The mime sequence in pBR322 was selected to have similar melting and annealing characteristics to that of the sGC subunit sequence being probed. The semiquantitative assessment of mRNA for each sGC subunit demonstrated low variability across multiple total RNA preparations and close agreement in the amount of mRNA measured for both sGC subunits in both tissues. Taken together these precautions and findings suggest that random differences in reverse transcription efficiency within and across tissues did not contribute significantly to the measurement of sGC subunit mRNA expression. The possibility of a systematic error due to

use of a cDNA mime and reverse transcribed mRNA from tissue total RNA samples still exists and cannot be addressed with the methods used. Thus the values for sGC subunit mRNA expression reported in these studies are best taken as a precise lower limit.

The recent finding that homodimers of sGC subunits (e.g., $sGC\beta_1/sGC\beta_1$) can occur (48) suggests another mechanism by which sGC expression might be regulated differently in two tissues, despite expression of the same sGC subunits. Unequal expression of the two sGC subunits would result in formation of either a fraction of inactive (48) or less active (26) sGC homodimer with the amount of active homodimer limited by the less abundantly expressed sGC subunit. In the present studies PASM expression of $sGC\alpha_1$ and $sGC\beta_1$ subunits was higher than in TSM and approximately equal, suggesting that greater sGC activity in PASM is due, in part, to greater mRNA expression of both sGC subunits. In TSM, $sGC\alpha_1$ was less than $sGC\beta_1$ subunit mRNA expression, suggesting the possibility of $sGC\beta_1$ homodimer formation in this tissue. A similar observation of greater $sGC\beta_1$ mRNA expression has been previously reported in vascular smooth muscle (25), but verification of this at the level of sGC subunit protein expression and direct demonstration of $sGC\beta_1$ homodimer formation in a fully differentiated smooth muscle tissue awaits further investigation.

In the absence of purified sGC subunit protein standards, it was not possible to assess the specificity of commercially available antibodies. sGC purified from bovine lung was used as a protein standard, and a commercially available antibody that was generated against antigenic peptides from both $sGC\alpha_1$ and $sGC\beta_1$ was successfully used to detect sGC in canine PASM and TSM. The method used in these studies to semiquantitatively determine sGC protein expression involved the use of a protein standard, in this case purified bovine lung sGC heterodimer to generate a standard curve. The amount of sGC present in tissue homogenates was then determined using this standard curve and interpolation, in a manner analogous to a Bradford protein assay using a purified form of a protein as its own standard. The amount of sGC used in the standard curve was designed to ensure that the chemiluminescent signal from sGC in tissue homogenates was in the midrange of the standard curve. This is the first report of the amount of sGC protein expressed in smooth muscle tissue. The amount sGC in the soluble fraction of tissue homogenates reported here is significantly lower than that reported in rat brain (35), which may be due to differences in tissue and/or species and the fact that sGC concentration in the latter study was determined by only a single sGC protein standard concentration, rather than a standard curve.

The commercially available sGC antibody used is described as specific to $sGC\beta_1$, and the antigenic peptide sequence used to generate this rabbit polyclonal antibody is identical across all mammalian species, including dog. It is therefore improbable that use of the bovine lung sGC protein standard resulted in a species-related difference in the anti-sGC antibody binding to sGC in bovine vs. canine protein. A potential source of error that cannot be accounted for with the methods used is that the amount of sGC protein present in the commercially available protein sample may be higher than described on the package insert by as much as a factor of two. This would result in an underestimation of the amount of sGC present in the canine PASM and TSM tissue homogenates and would be a source of error that would have an equal effect in both tissues. The greater sGC protein found in PASM vs. TSM suggests that most of the difference in sGC activity between the tissues is accounted for by greater sGC expression, rather than greater sGC-specific activity in PASM.

In summary, the present study demonstrates that relaxation to NO in both PASM and TSM is attributable to both cGMP and cGMP-dependent protein kinase mechanisms. This is true for NO-mediated relaxation of submaximal and maximal contractions induced by either receptor-agonists or membrane depolarization. Thus mechanisms intrinsic to smooth muscle contribute significantly to the clinical finding of apparently greater NO responsiveness in pulmonary vasculature vs. airways. The amount of cGMP under steady-state conditions was greater in PASM than in TSM at a given NO concentration. Differences in PDE activity plays little role in the greater NO responsiveness of PASM. The only sGC subunits expressed in significant amounts in PASM and TSM, $sGC\alpha_1$ and $sGC\beta_1$, were both more abundantly expressed in PASM than in TSM, and this difference in expression appears to account for the greater cGMP production in PASM. Another mechanism that might contribute significantly to differences in the NO responsiveness between these tissues, differences in the responsiveness of the contractile system to the actions of cGMP, is not addressed in these studies.

ACKNOWLEDGMENTS

We thank Kathy Street and Susan Kost for expert technical assistance.

GRANTS

This work was supported by National Heart, Lung, and Blood Institute Grants HL-69968 (W. J. Perkins) and HL-54757 (K. A. Jones) and funds from Mayo Clinic College of Medicine.

REFERENCES

1. **Archer SL, Huang JM, Hampl V, Nelson DP, Shultz PJ, and Weir EK.** Nitric oxide and cGMP cause vasorelaxation by activation of a charybdotoxin-sensitive K channel by cGMP-dependent protein kinase. *Proc Natl Acad Sci USA* 91: 7583–7587, 1994.
2. **Becker-Andre M and Hahlbrock K.** Absolute mRNA quantification using the polymerase chain reaction (PCR). A novel approach by a PCR aided transcript titration assay (PATTY). *Nucleic Acids Res* 17: 9437–9446, 1989.
3. **Bellamy TC, Wood J, Goodwin DA, and Garthwaite J.** Rapid desensitization of the nitric oxide receptor, soluble guanylyl cyclase, underlies diversity of cellular cGMP responses. *Proc Natl Acad Sci USA* 97: 2928–2933, 2000.
4. **Black SM, Sanchez LS, Mata-Greenwood E, Bekker JM, Steinhorn RH, and Fineman JR.** sGC and PDE5 are elevated in lambs with increased pulmonary blood flow and pulmonary hypertension. *Am J Physiol Lung Cell Mol Physiol* 281: L1051–L1057, 2001.
5. **Buechler WA, Nakane M, and Murad F.** Expression of soluble guanylate cyclase activity requires both enzyme subunits. *Biochem Biophys Res Commun* 174: 351–357, 1991.
6. **Buga GM, Gold ME, Wood KS, Chaudhuri G, and Ignarro LJ.** Endothelium-derived nitric oxide relaxes nonvascular smooth muscle. *Eur J Pharmacol* 161: 61–72, 1989.
7. **Carter TD, Bettache N, and Ogden D.** Potency and kinetics of nitric oxide-mediated vascular smooth muscle relaxation determined with flash photolysis of ruthenium nitrosyl chlorides. *Br J Pharmacol* 122: 971–973, 1997.
8. **Chirgwin JM, Przybyla AE, MacDonald RJ, and Rutter WJ.** Isolation of biologically active ribonucleic acid from sources enriched in ribonuclease. *Biochemistry* 18: 5294–5299, 1979.
9. **Dhanakoti SN, Gao Y, Nguyen MQ, and Raj JU.** Involvement of cGMP-dependent protein kinase in the relaxation of ovine pulmonary arteries to cGMP and cAMP. *J Appl Physiol* 88: 1637–1642, 2000.

10. **Felbel J, Trockur B, Ecker T, Landgraf W, and Hofmann F.** Regulation of cytosolic calcium by cAMP and cGMP in freshly isolated smooth muscle cells from bovine trachea. *J Biol Chem* 263: 16764–16771, 1988.
11. **Filippov G, Bloch DB, and Bloch KD.** Nitric oxide decreases stability of mRNAs encoding soluble guanylate cyclase subunits in rat pulmonary artery smooth muscle cells. *J Clin Invest* 100: 942–948, 1997.
12. **Gao Y, Dhanakoti S, Tolsa JF, and Raj JU.** Role of protein kinase G in nitric oxide- and cGMP-induced relaxation of newborn ovine pulmonary veins. *J Appl Physiol* 87: 993–998, 1999.
13. **Geiselhoringer A, Werner M, Sigl K, Smital P, Worner R, Acheo L, Stieber J, Weinmeister P, Feil R, Feil S, Wegener J, Hofmann F, and Schlossmann J.** IRAG is essential for relaxation of receptor-triggered smooth muscle contraction by cGMP kinase. *EMBO J* 23: 4222–4231, 2004.
14. **Gibb BJ, Wykes V, and Garthwaite J.** Properties of NO-activated guanylyl cyclases expressed in cells. *Br J Pharmacol* 139: 1032–1040, 2003.
15. **Giembycz MA and Raeburn D.** Putative substrates for cyclic nucleotide-dependent protein kinases and the control of airway smooth muscle tone. *J Auton Pharmacol* 11: 365–398, 1991.
16. **Gilliland G, Perrin S, Blanchard K, and Bunn HF.** Analysis of cytokine mRNA and DNA: detection and quantitation by competitive polymerase chain reaction. *Proc Natl Acad Sci USA* 87: 2725–2729, 1990.
17. **Giuili G, Scholl U, Bulle F, and Guellaen G.** Molecular cloning of the cDNAs coding for the two subunits of soluble guanylyl cyclase from human brain. *FEBS Lett* 304: 83–88, 1992.
18. **Hobbs AJ and Ignarro LJ.** Nitric oxide-cyclic GMP signal transduction system. *Methods Enzymol* 269: 134–148, 1996.
19. **Hogman M, Frostell CG, Hedenstrom H, and Hedenstierna G.** Inhalation of nitric oxide modulates adult human bronchial tone. *Am Rev Respir Dis* 148: 1474–1478, 1993.
20. **Jones KA, Lorenz RR, Morimoto N, Sieck GC, and Warner DO.** Halothane reduces force and intracellular Ca^{2+} in airway smooth muscle independently of cyclic nucleotides. *Am J Physiol Lung Cell Mol Physiol* 268: L166–L172, 1995.
21. **Kacmarek RM, Ripple R, Cockrill BA, Bloch KJ, Zapol WM, and Johnson DC.** Inhaled nitric oxide. A bronchodilator in mild asthmatics with methacholine-induced bronchospasm. *Am J Respir Crit Care Med* 153: 128–135, 1996.
22. **Keefer LK.** Progress toward clinical application of the nitric oxide-releasing diazeniumdiolates. *Annu Rev Pharmacol Toxicol* 43: 585–607, 2003.
23. **Keefer LK, Nims RW, Davies KM, and Wink DA.** "NONOates" (1-substituted diazen-1-ium-1,2-diolates) as nitric oxide donors: convenient nitric oxide dosage forms. *Methods Enzymol* 268: 281–293, 1996.
24. **Kennedy T, Summer WR, Sylvester J, and Robertson D.** Airway response to sublingual nitroglycerin in acute asthma. *JAMA* 246: 145–147, 1981.
25. **Kloss S, Furneaux H, and Mulsch A.** Post-transcriptional regulation of soluble guanylyl cyclase expression in rat aorta. *J Biol Chem* 278: 2377–2383, 2003.
26. **Koglin M, Vehse K, Budaeus L, Scholz H, and Behrends S.** Nitric oxide activates the beta 2 subunit of soluble guanylyl cyclase in the absence of a second subunit. *J Biol Chem* 276: 30737–30743., 2001.
27. **Kreye VA and Marquard E.** Comparison of sodium nitroprusside and isoprenaline aerosols in histamine-induced bronchial asthma of the guinea pig. *Naunyn Schmiedebergs Arch Pharmacol* 306: 203–207, 1979.
28. **Lowry AH, Rosebrough NJ, Farr AL, and Randall RJ.** Protein measurement with the Folin reagent. *J Biol Chem* 193: 265–275, 1951.
29. **Maclean MR, Johnston ED, McCulloch KM, Pooley L, Houslay MD, and Sweeney G.** Phosphodiesterase isoforms in the pulmonary arterial circulation of the rat: changes in pulmonary hypertension. *J Pharmacol Exp Ther* 283: 619–624., 1997.
30. **Maragos CM, Morley D, Wink DA, Dunams TM, Saavedra JE, Hoffman A, Bove AA, Isaac L, Hrabie JA, and Keefer LK.** Complexes of NO with nucleophiles as agents for the controlled biological release of nitric oxide. Vasorelaxant effects. *J Med Chem* 34: 3242–3247, 1991.
31. **Meddings JB, Scott RB, and Fick GH.** Analysis and comparison of sigmoidal curves: application to dose-response data. *Am J Physiol Gastrointest Liver Physiol* 257: G982–G989, 1989.
32. **Moro MA, Russell RJ, Cellek S, Lizasoain I, Su YC, Darleyusmar VM, Radomski MW, and Moncada S.** cGMP mediates the vascular and platelet actions of nitric oxide - confirmation using an inhibitor of the soluble guanylyl cyclase. *Proc Natl Acad Sci USA* 93: 1480–1485, 1996.
33. **Murad F.** Regulation of cytosolic guanylyl cyclase by nitric oxide: The NO-cyclic GMP signal transduction system. In: *Cyclic GMP: Synthesis, Metabolism, and Function*, edited by Murad F. San Diego, CA: Academic, 1994, p. 19–33.
34. **Nakane M, Arai K, Saheki S, Kuno T, Buechler W, and Murad F.** Molecular cloning and expression of cDNAs coding for soluble guanylate cyclase from rat lung. *J Biol Chem* 265: 16841–16845, 1990.
35. **Nedvetsky PI, Kleinschnitz C, and Schmidt HH.** Regional distribution of protein and activity of the nitric oxide receptor, soluble guanylyl cyclase, in rat brain suggests multiple mechanisms of regulation. *Brain Res* 950: 148–154, 2002.
36. **Nishikawa M, de Lanerolle P, Lincoln TM, and Adelstein RS.** Phosphorylation of mammalian myosin light chain kinases by the catalytic subunit of cyclic AMP-dependent protein kinase and by cyclic GMP-dependent protein kinase. *J Biol Chem* 259: 8429–8436, 1984.
37. **Pabelick CM, Warner DO, Perkins WJ, and Jones KA.** *S*-nitrosoglutathione-induced decrease in calcium sensitivity of airway smooth muscle. *Am J Physiol Lung Cell Mol Physiol* 278: L521–L527, 2000.
38. **Pauvert O, Salvail D, Rousseau E, Lugnier C, Marthan R, and Savineau JP.** Characterisation of cyclic nucleotide phosphodiesterase isoforms in the media layer of the main pulmonary artery. *Biochem Pharmacol* 63: 1763–1772, 2002.
39. **Perkins WJ, Pabelick C, Warner DO, and Jones KA.** cGMP-independent mechanism of airway smooth muscle relaxation induced by S-nitrosoglutathione. *Am J Physiol Cell Physiol* 275: C468–C474, 1998.
40. **Rho EH, Perkins WJ, Lorenz RR, Warner DO, and Jones KA.** Differential effects of soluble and particulate guanylyl cyclase on Ca^{2+} sensitivity in airway smooth muscle. *J Appl Physiol* 92: 257–263, 2002.
41. **Sanger F, Nicklen S, and Coulson AR.** DNA sequencing with chain-terminating inhibitors. *Proc Natl Acad Sci USA* 74: 5463–5467, 1977.
42. **Somlyo AP and Somlyo AV.** Ca^{2+} sensitivity of smooth muscle and nonmuscle myosin II: modulated by G proteins, kinases and myosin phosphatase. *Physiol Rev* 83: 1325–1358, 2003.
43. **Stuart-Smith K, Bynoe TC, Lindeman KS, and Hirshman CA.** Differential effects of nitrovasodilators and nitric oxide on porcine tracheal and bronchial muscle in vitro. *J Appl Physiol* 77: 1142–1147, 1994.
44. **Torphy TJ, Undem BJ, Cieslinski LB, Luttmann MA, Reeves ML, and Hay DW.** Identification, characterization and functional role of phosphodiesterase isozymes in human airway smooth muscle. *J Pharmacol Exp Ther* 265: 1213–1223, 1993.
45. **Waniishi Y, Inoue R, Morita H, Teramoto N, Abe K, and Ito Y.** Cyclic GMP-dependent but G-kinase-independent inhibition of Ca^{2+}-dependent Cl^- currents by NO donors in cat tracheal smooth muscle. *J Physiol* 511: 719–731, 1998.
46. **Wedel B, Humbert P, Harteneck C, Foerster J, Malkewitz J, Bohme E, Schultz G, and Koesling D.** Mutation of His-105 in the beta 1 subunit yields a nitric oxide-insensitive form of soluble guanylyl cyclase. *Proc Natl Acad Sci USA* 91: 2592–2596, 1994.
47. **Wernet W, Flockerzi V, and Hofmann F.** The cDNA of the two isoforms of bovine cGMP-dependent protein kinase. *FEBS Lett* 251: 191–196, 1989.
48. **Zabel U, Hausler C, Weeger M, and Schmidt HH.** Homodimerization of soluble guanylyl cyclase subunits. Dimerization analysis using a glutathione s-transferase affinity tag. *J Biol Chem* 274: 18149–18152, 1999.
49. **Zabel U, Weeger M, La M, and Schmidt HH.** Human soluble guanylate cyclase: functional expression and revised isoenzyme family. *Biochem J* 335: 51–57, 1998.
50. **Zhou HL and Torphy TJ.** Relationship between cyclic guanosine monophosphate accumulation and relaxation of canine trachealis induced by nitrovasodilators. *J Pharmacol Exp Ther* 258: 972–978, 1991.